

# Long-Term Deposit Formation in Aviation Turbine Fuel at Elevated Temperature

A.J. Giovanetti\* and E.J. Szetela†

*United Technologies Research Center, East Hartford, Connecticut*

An experimental research program was undertaken to characterize the relationship between deposit mass, operating time, and temperature in coking studies for aviation fuels under conditions simulating those for a modern turbine aircraft fuel system. The rates of carbon deposition were determined for Jet A and the alternative fuel Suntech A flowing in heated stainless steel tubes for tube temperatures in the range of 420-750 K, test durations of 3-730 h, and at fuel velocities of 0.07 and 1.3 m/s. In general, deposit rates were found to be a strong function of tube temperature and, at common test condition, the rates for Suntech A exceeded those for Jet A by a factor of 10. Unexpectedly, for both fuels, deposit rates increased markedly as the test duration increased. Also, all deposits obtained at the low-velocity condition of 0.07 m/s were nonuniform in thickness and cellular in structure and found to have an average density of 0.08 g/cm<sup>3</sup> based on carbon content. However, for the higher velocity of 1.3 m/s, coverage of the tube by deposit was more uniform and an average deposit density equal to 0.8 g/cm<sup>3</sup> was measured. In addition, the heated tube data were used to develop a global chemical kinetic model for fuel oxidation and carbon deposition. When applied to the experiment, the model verified the effect of dissolved oxygen in the fuel as a limiting agent for deposit formation.

## Nomenclature

$A$	= experimentally determined reaction constant, cm <sup>3</sup> /mole·s
$E$	= Arrhenius activation energy, cal/mole
$k$	= specific reaction rate constant, cm <sup>3</sup> /mole·s
$Q/A$	= heat flux applied to tube, W/cm <sup>2</sup>
$R$	= universal gas constant, 1.987 cal/g·mole·K
$T$	= temperature, K
$t$	= time, s

## Subscripts

$n$	= reaction number
$0$	= initial
$[ ]$	= concentration, moles/cm <sup>3</sup>

## Introduction

**H**YDROCARBON gas turbine fuels in contact with heated metallic surfaces form insoluble, carbonaceous deposits that can plug fuel passages in heat exchangers, manifolds, and injectors. Although there is presently only a limited understanding of the chemical mechanisms responsible for fuel thermal degradation, it is believed that the deposit formation process involves oxidation and pyrolysis of hydrocarbon fuel molecules and the formation of free-radical species. This degradation is often aided by the presence of fuel impurities such as metals, sulfur, and nitrogen. These intermediate species undergo further reaction to form higher molecular weight materials that usually contain carbon, hydrogen, oxygen, sulfur, and nitrogen.

In an earlier companion paper, deposit data were presented from experiments with Jet A aviation fuel flowing

through electrically heated tubes.<sup>1</sup> In these experiments, parametric tests to map the fuel deposition characteristics of Jet A were conducted to simulate the filming region of an advanced aircraft air blast nozzle. The important test conditions included a pressure of 3.4 MPa, a fuel velocity of 0.07 m/s (flow rate of 0.73 kg/h), tube wall temperatures in the range of 420-630 K, maximum fuel temperatures in the range of 420-560 K, and for test durations of 3-730 h. The longest duration heated tube tests previously reported<sup>2,3</sup> were run for 106 h at temperatures of 485-580 K and for 100 h at temperatures of 745-1000 K. The results reported herein indicate that the carbon deposit rates were a strong function of tube wall temperature. Unexpectedly, at a fixed value of tube temperature, the deposition rates were proportional to approximately the second power of the test duration, i.e., the time-averaged deposition rates quadrupled as the test time doubled. One explanation for this trend with operating time was that it was due to the active surface provided by the cellular structure of the deposit formed on the tube wall during early stages of the test. The average density of the deposit in these experiments at all of the test durations measured was 0.08 g/cm<sup>3</sup> based on carbon content.

Also, in individual tests where the fuel residence time was sufficiently long at elevated tube temperatures, deposit rates reached maximum values at intermediate values of tube temperature and position. As the fuel residence time and tube temperature were further increased, the deposit rates decreased significantly from their maximum values. A possible explanation for this phenomenon was that, during the fuel heating process, active oxygenated species (which are precursors to deposit formation) are formed and later depleted as the fuel flows through the tube.

The purpose of this paper is to extend the data base begun earlier by adding data from tests with Jet A conducted at a higher velocity (1.3 m/s) to simulate the operation of the nozzle at a high-thrust condition and from tests using the alternative fuel Suntech A, which was selected by the Navy as an example of a lower-quality gas turbine fuel. In addition, the predictions of a well-stirred reactor model of the heated tube experiment employing a two-step chemical reaction mechanism of fuel oxidation and deposit formation are

Presented as Paper 85-0525 at the AIAA 24th Aerospace Sciences Meeting, Reno, NV, Jan. 6-9, 1986; received Jan. 22, 1986; revision received April 14, 1986. Copyright © American Institute of Aeronautics and Astronautics, Inc., 1986. All rights reserved.

\*Research Engineer (currently with General Electric Co., Pittsfield, MA).

†Senior Research Engineer.

presented and compared to the experimental data. In a concise manner, the model relates the heated tube data for a range of surface temperatures, fuel residence times, fuel velocities, and test durations. Ultimately, this information can be incorporated into a design algorithm for use in predicting coking rates in fuel system components under service conditions.

## Apparatus and Test Procedures

### Apparatus

A novel fuel thermal stability test apparatus, shown schematically in Fig. 1, was developed to provide fundamental information on fuel deposition rates over a wide range of temperatures, test durations, and flow rates.<sup>1</sup> The apparatus consists of a test section comprising three, resistance-heated 0.91 m long, 0.22 cm i.d.  $\times$  0.32 cm o.d., 316 stainless steel tubes, each of which is connected in series to a downstream 0.30 m long, unheated constant-temperature (isothermal) tube having an identical cross section. Because of the planned long-duration tests and the considerable effort required to run them, multiple tubes were chosen to permit tests of different durations to be run concurrently. The resistance heated tubes are brazed to copper electrodes attached to an 8 kVA ac power supply and the connecting isothermal tubes are enclosed in cylindrical ceramic ovens to compensate for heat losses to the environment. Chromel-alumel thermocouples are spot welded to the outer surface of each tube at prescribed intervals for accurate surface temperature determination; duplicate thermocouples inserted into the fuel stream to measure the fuel inlet and outlet temperatures. In addition, 316 stainless steel wafer specimens (0.64 cm long  $\times$  0.32 cm wide  $\times$  0.005 cm thick) are immersed in the fuel stream at locations immediately upstream and downstream of each isothermal tube section. The heated tube sections provide information on the deposit formation that occurs when the temperature differential between the surface and fuel is large (approximately 100 K), whereas the isothermal tubes and metal wafer specimens yield data for the condition in which the surface and fuel temperatures are equal.

The test tube assemblies are electrically isolated, mounted vertically, and wrapped in blankets of Fiberfrax insulation to reduce heat losses. The vertical orientation causes the buoyancy forces acting on the fuel (due to the induced axial temperature gradient) to be in the same direction as the flow, thereby suppressing any secondary flow motion that would occur at laminar flow conditions having low Reynolds numbers. During each three-tube test, the fuel inlet and outlet temperatures for each tube are held constant using a proportional temperature controller and solid-state power relay. An electrically driven fuel metering valve responds to the output of the turbine flow meter and regulates the total flow rate through the test section, whereas the metering orifices located at the inlet of the tubes assure identical flow rates between the tubes. All apparatus control systems are coupled to an interlock system and all pressure, temperature, electrical power, and flow rate data are recorded automatically with a calculating data logger microprocessor that provides for safe, unattended operation.

### Deposit Characterization

The quantity of carbon deposited in each tube is measured by cutting the tube into sections, oxidizing the deposit on each of these sections in a stream of oxygen, collecting the effluent gases in evacuated flasks, and measuring the concentrations of CO<sub>2</sub> in the gases using nondispersive infrared analyzers. Prior to analysis, the tube specimens are vacuum dried at 370 K for about 12 h to remove any residual liquid fuel. The minimum mass of carbon that can be determined accurately using the oxidation method is 200  $\mu$ g.

The carbon mass, determined from the deposit oxidation analysis technique, is used to compute the normalized rate of carbon deposition, which is defined as the mass of carbon divided by the surface area of the specimen and the total test time. (The deposition is expressed in units of  $\mu$ g/cm<sup>2</sup>·h.) In the case of tube specimens where the accumulation of deposit on the tube wall reduces the inside lateral surface area, an average of the clean tube area and final surface area wetted by the fuel is used in calculating the carbon deposition rate.

### Fuel Characterizations

Each of the two fuels used in the program was withdrawn as a single batch from a large supply and stored in unused steel drums under an unheated protective enclosure. The Jet A (ASTM D 1655) was acquired from a local gas turbine development facility and the alternative fuel, Suntech A, was supplied by the U.S. Naval Air Propulsion Center. A series of analyses were conducted for each fuel to quantify its chemical composition and thermal stability characteristics. In general, the Suntech A exhibited higher mass concentrations of fuel impurities with respect to the Jet A (e.g., 0.24% sulfur compared to 0.05% and 250 ppm nitrogen compared to 12 ppm) and it had a total aromatic content of 40% by volume compared to 21%. Because of the relatively high concentrations of sulfur and nitrogen, as well as the greater fraction of aromatic hydrocarbons present in the Suntech A, it was expected that its jet fuel thermal oxidation tester (JFTOT) breakpoint temperature as measured using the ASTM D 3241 test procedure would be lower (i.e., poor thermal stability) than that for the Jet A. However, the actual values for the Suntech A and Jet A were determined to be 538 and 529 K, respectively. The apparent anomaly between the breakpoint temperature and the fuel characteristics may be related to the observation that the Suntech fuel has exhibited considerable timewise variation in breakpoint temperature; this behavior has been the object of continuing investigations.

All of the fuel used in the experimental program was filtered on-line through a 2  $\mu$ m porosity fuel filter prior to injection into the heated tube test section. In addition, because the effects of dissolved oxygen on fuel thermal stability are known to be important and in order to establish a repeatable baseline concentration that approximates the condition of normal use, each fuel was saturated with filtered air immediately prior to test using an inline sintered steel sparging element. See Fig. 1.

## Experimental Results and Discussion

The test conditions were chosen to provide a data base for fuel deposition in internal flow passages under forced convec-

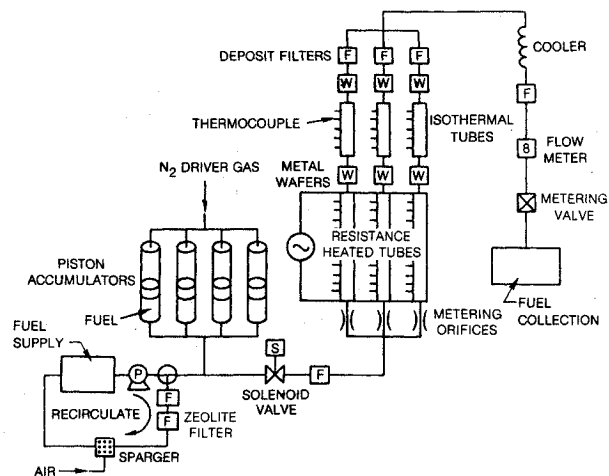


Fig. 1 Fuel deposit test apparatus.

tive conditions simulating the environment of a modern aviation gas turbine fuel system. Individual tests were designed to elucidate the effects of wall temperature, fuel velocity, fuel residence time during heating, and total test (operating) time.

Deposit Structure

The distinct characteristics of the Jet A fuel deposits obtained as a function of fuel velocity are shown photographically in Fig. 2. Shown here are two transverse sections of tube run at different fuel velocities and the deposits formed on them after 20 h of operation at a surface temperature of approximately 580 K. As shown in Fig. 2 and reported in Ref. 1, the deposit formed at the low-velocity (0.07 m/s) condition appears to be cellular, with an irregular structure that could be described as filamentous. Similarly, the deposit formed on the tubes run with Suntech A at low velocity (not shown) was also characterized by an irregular, cellular structure. However, for the high-velocity (1.3 m/s) condition shown in Fig. 2, the coverage of the tube surface by the deposits is more uniform and appears amorphous. The higher wall shear associated with the high-velocity condition may suppress the growth of the cellular deposit characteristic at low velocity. Using Fig. 2 to estimate the average deposit thicknesses at these conditions, together with the deposit mass loading information determined from the oxidation analyses, the average deposit densities (based on carbon content) for the low- and high-velocity conditions are 0.08 and 0.8 g/cm<sup>3</sup>, respectively.

Fuel Deposition at Low Velocity

Using the deposit oxidation analysis procedure described above, the rates of carbon deposition were evaluated for a large number of tube specimens taken from tests run for Jet A and Suntech A fuels. A summary of the smoothed time-averaged rates of carbon deposition for Jet A at low velocity (0.07 m/s) as a function of initial wall temperature and test duration is shown in Fig. 3. Only data from the heated tube

portion of the experiment is shown. The selection of initial wall temperature as the correlating parameter assumes that the initial clean-tube wall temperature equals the temperature at the interface between the fuel and deposit layer because the applied heat flux and fuel flow rate are constant with time. Also, because the wall temperature is proportional to the distance from the heated tube inlet, Fig. 3 can be thought of as a plot of the deposit rate vs the axial position along the tube.

As shown in Fig. 3 for tests in which the maximum tube temperature was above 500 K, the rates of carbon deposition increase to a peak value with increasing tube wall temperature (position) in the range of 425-550 K. At temperatures above 550 K, the deposit rates decrease from their peak values. The reasons for the shape of the curve have not been established with certainty, but it is believed that, as the fuel is heated, active oxygenated species such as hydroperoxides (which are precursors to deposit formation) are formed and depleted as the fuel flows through the tube. Also, if the dissolved oxygen concentration in the fuel, the tube wall temperature, and the

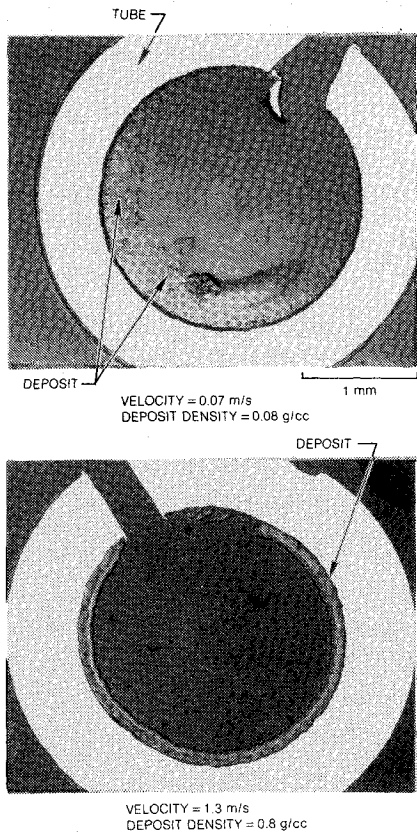


Fig. 2 Effect of fuel velocity on deposit structure (Jet A, 580 K, 20 h test duration).

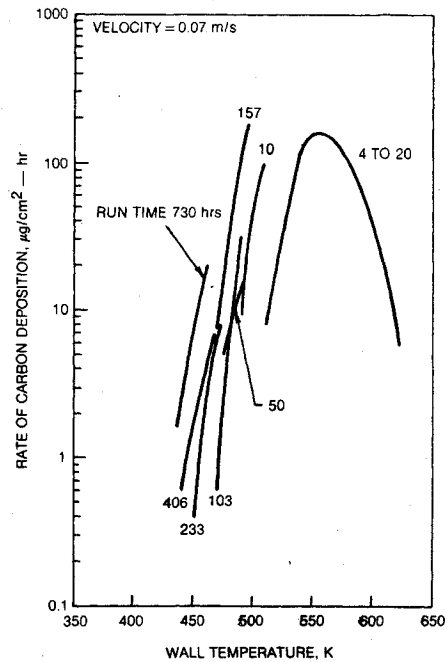


Fig. 3 Carbon deposition rate for Jet A at low velocity (from Ref. 1).

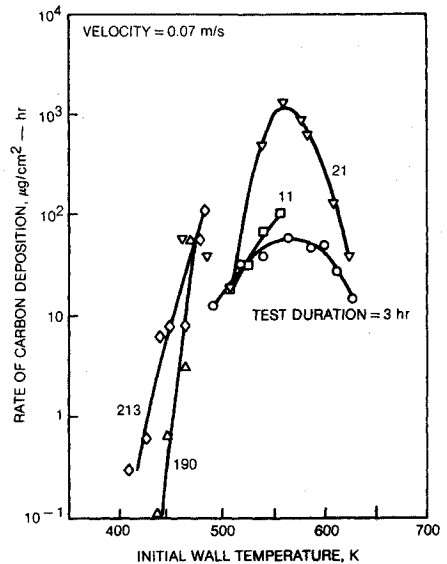


Fig. 4 Carbon deposition rate for Suntech A at low velocity.

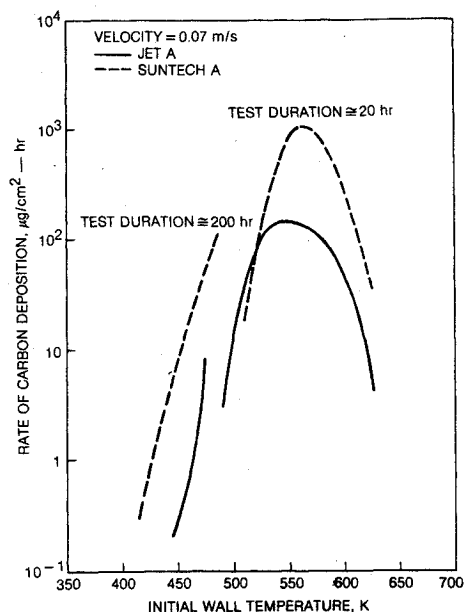


Fig. 5 Comparison of rates for Jet A and Suntech A.

fuel residence time during heating are sufficiently high, a maximum will occur in the deposit rate vs temperature relationship.

The effect of the test duration on the deposit rates is also evident in Fig. 3, which shows an apparent increase in the rates of carbon deposition for a fixed value of the wall temperature as the test duration increases, i.e., the total deposit produced does not scale linearly with the test duration. In fact, Fig. 3 indicates that the deposit rate approximately increases with the second power of the test time. One possible explanation for this nonlinear behavior is that the deposit surface may become active and result in a rapid increase in the deposited mass.<sup>1</sup> However, a question arises as to whether this apparent nonlinear relationship between the deposit formation and the test time is affected by the manner in which the data are plotted. Earlier, it was postulated that the initial tube temperature is the appropriate correlating parameter because, when the applied heat flux and fuel flow rate are maintained constant, the temperature at the interface between the fuel and deposit formed is always equal to the initial clean-tube wall temperature. This contention is valid only for the formation of nonporous, thin uniform deposits and where all additional deposits develop on the exposed surface. This postulation is not valid for the thick, highly cellular deposits (such as those observed in the low-velocity experiments) having significant internal temperature gradients. Because the surface temperature of the deposit adjacent to the tube wall is rising with time (due to the increase in the thermal resistance from the accumulation of the deposit), the additional deposit that forms in the stagnant fuel trapped in the void volumes of a porous deposit may be produced at an effective temperature significantly greater than the initial wall value. Therefore, the apparent trend of an increasing rate of carbon deposition with the initial wall temperature shown in Fig. 3 is not significant if the actual temperature governing the deposit formation is nearer in magnitude to the inside tube wall temperature.<sup>4</sup>

The carbon deposition rates for Suntech A at low velocity are plotted in Fig. 4 and a comparison of the deposition rates for similar tests using Jet A and Suntech A is shown in Fig. 5. In general, the trends displayed in the data for Suntech A are similar to those of Jet A, except that the deposition rates for Suntech A can be as high as a factor of 10 greater. Also, as for Jet A, a maximum in the carbon deposition vs wall temperature curve occurs at about 560 K.

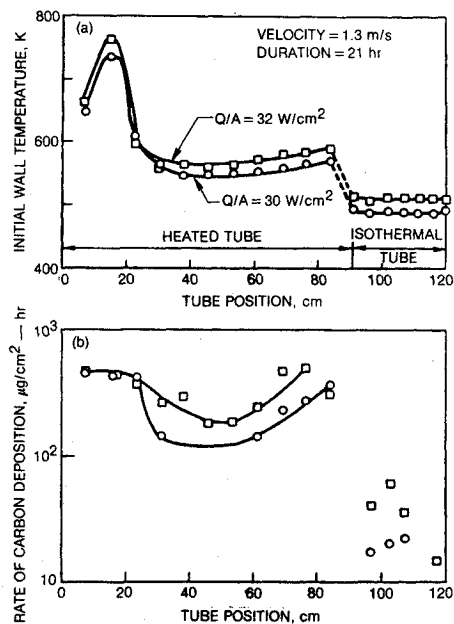


Fig. 6 Carbon deposition rate for Jet A at high velocity.

#### Rates of Carbon Deposition at High Velocity

The deposit data for the high-velocity (1.3 m/s) and short-duration tests using Jet A is plotted in Fig. 6. Because of the nonmonotonic heated tube wall temperature profiles caused by tube entrance effects that result in two different tube positions having an identical wall temperature (see Fig. 6a), the deposit rate and cumulative carbon deposit data are plotted as a function of the tube position to permit differentiation of the upstream and downstream temperatures. Isothermal tube data are also plotted for tube positions between 96 and 120 cm. In Fig. 6b, the deposit rates are monotonically increasing with the tube position in the regions of monotonically increasing wall temperature, which suggests that the depletion of active oxygenated species does not occur when the fuel residence time in heating is short (less than 1 s at this velocity condition). In fact, in Fig. 6b, the magnitude of the deposit rates at high velocity are similar to those at the low-velocity condition shown earlier in Fig. 3 at the common test condition of an initial wall temperature of 550 K (rates approximately equal to  $150 \mu\text{g}/\text{cm}^2 \cdot \text{h}$ ). However, in the high-velocity runs at wall temperatures greater than 550 K and for tube positions downstream of 60 cm, the deposit rates are higher than those for the low-velocity test at comparable wall temperatures. This comparison between the low- and high-velocity deposition data at similar wall temperatures reinforces the importance of the fuel temperature-time history in affecting downstream deposition and the need to interpret deposit data considering this effect.

#### Fuel Oxidation and Deposition Model

The detailed chemical reactions that result in fuel deposits are very complex and not well understood at present. It is widely agreed, however, that at temperatures up to about 540 K (the principal region of interest in this investigation), they usually begin with a liquid-phase auto-oxidation of the fuel, which is promoted by dissolved oxygen.<sup>5</sup> Further, Hazlett<sup>6</sup> has identified the important deposit-forming precursor species in his studies of reactions of aerated n-dodecane flowing over heated stainless steel tubes. Using gas chromatography, he chemically analyzed the stressed fuel sample discharged from a JFTOT. Some results are shown in Fig. 7, where the concentrations of oxygenated species (hydroperoxides, alcohols, ketones, and carbon monoxide) are related to a light-reflectance measurement of the deposit formed on the tube

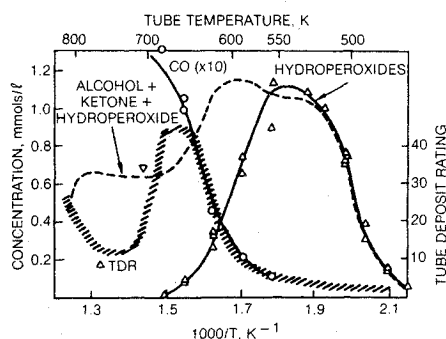
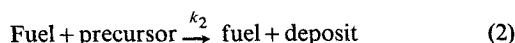
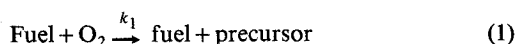


Fig. 7 Oxygenated compounds from n-Dodecane.

known as the tube deposit rating ( $\Delta TDR$ ). The data in Fig. 7 suggest that deposit formation (as characterized by  $\Delta TDR$ ) is closely related to the formation of oxygenated intermediary precursor species.

Based on the trends shown in the data of Fig. 7, it is reasonable to postulate the following global two-step kinetic reaction mechanism:



where the time rates of change of the active species are given by

$$\frac{d[\text{O}_2]}{dt} = -k_1 [\text{fuel}] [\text{O}_2] \quad (3)$$

$$\frac{d[\text{deposit}]}{dt} = k_2 [\text{fuel}] [\text{precursor}] \quad (4)$$

and

$$\frac{d[\text{precursor}]}{dt} = -\left(\frac{d[\text{O}_2]}{dt} + \frac{d[\text{deposit}]}{dt}\right) \quad (5)$$

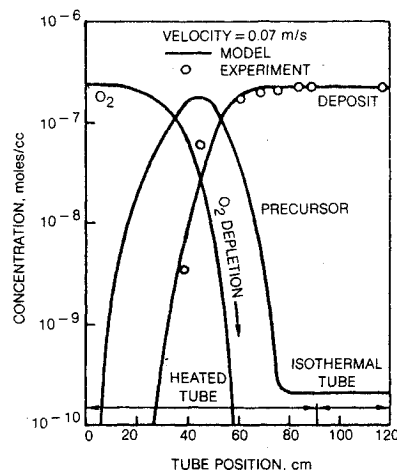
The brackets  $[\ ]$  denote concentration in moles/cm<sup>3</sup> and, because the sum of the concentrations of the O<sub>2</sub>, precursor, and deposit species is small (a few parts per million with respect to the fuel), the fraction of the fuel converted to deposit is negligible and is treated as a constant in the system. Also, the specific reaction rate constants  $k_1$  and  $k_2$  take the Arrhenius form,

$$k_n = A_n \exp(-E_n/RT), \text{ cm}^3/\text{mole} \cdot \text{s} \quad (6)$$

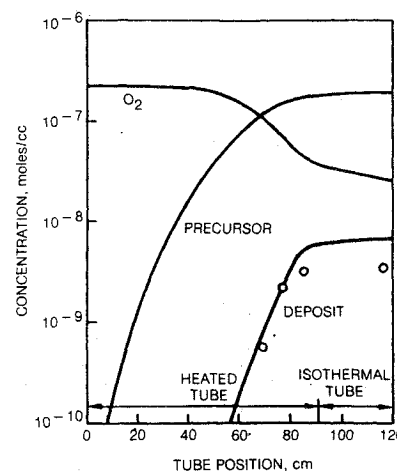
where  $A_n$  and  $E_n$  are the experimentally derived pre-exponential constants and activation energies, respectively,  $R$  the universal gas constant, and  $T$  the local tube temperature. Although it was found in many of the test runs that tube temperature was constant with time, thick deposits resulted in temperature gradients that were not taken into account.

Equations (1) and (2) require that, at any time during the reaction, the sum of the concentrations of the oxygen, precursor, and deposit is constant and equal to the initial concentration of oxygen,  $[\text{O}_2]_0$ , provided the initial concentrations of the precursor and deposit species are zero. Also, the reaction mechanism adopted permits the total production of deposit to be as high as  $[\text{O}_2]_0$  and, because of this, the value of  $[\text{O}_2]_0$  input to the model is chosen so that the predicted deposit matches experimental data. Of course, an upper limit on the  $[\text{O}_2]_0$  is the equilibrium value of dissolved oxygen in fully air-saturated fuel (about 55 ppm by weight or  $1.4 \times 10^{-6}$  moles O<sub>2</sub>/cm<sup>3</sup> fuel).

The values of the pre-exponential constants and activation energies required in Eq. (6) for each reaction were obtained



a) High-temperature condition.



b) Low-temperature condition.

Fig. 8 Predicted and measured deposit species concentration for Jet A.

by solving Eqs. (3) and (4) for the specific reaction rates  $k_1$  and  $k_2$  and plotting each against the reciprocal temperature on semilogarithmic graph paper from which the average slope  $E_n/R$  and intercept  $A_n$  were determined. Values for the concentrations of the individual species were approximated using selected data from Figs. 3 and 7. The values for the pre-exponential constants  $A_1$  and  $A_2$  were determined to equal  $3.5 \times 10^9$  and  $2.0 \times 10^{14}$  cm<sup>3</sup>/mole·s, respectively, and values for the activation energies  $E_1$  and  $E_2$  were estimated as 17 and 31 kcal/mole. The value for  $[\text{O}_2]_0$  was calibrated as  $2.25 \times 10^{-7}$  moles/cm<sup>3</sup> or 16% of the value for air-saturated fuel. A portion of the dissolved oxygen that did not participate in precursor-forming reaction was removed from the system in the form of inactive alcohols and ketones or as dissolved gas that did not diffuse to the tube wall. The molecular weight of the fuel was assumed equal to 170 g/mole and, because the deposit formation rate data are based on carbon mass rather than total mass, the molecular weight of deposit was assumed equal to that of carbon to permit a consistent comparison between the model predictions and the experiment.

Equations (3-5) were written in finite difference form and solved on a digital computer. The resultant computer program was applied to the heated and isothermal tube experiment by assuming that, at any station along either tube, the system is modeled as a well-stirred reactor maintained at the local tube temperature. The reactor volume equals the total volume of fuel passed through the tube during the test. The calculation proceeds by dividing the tube into finite in-

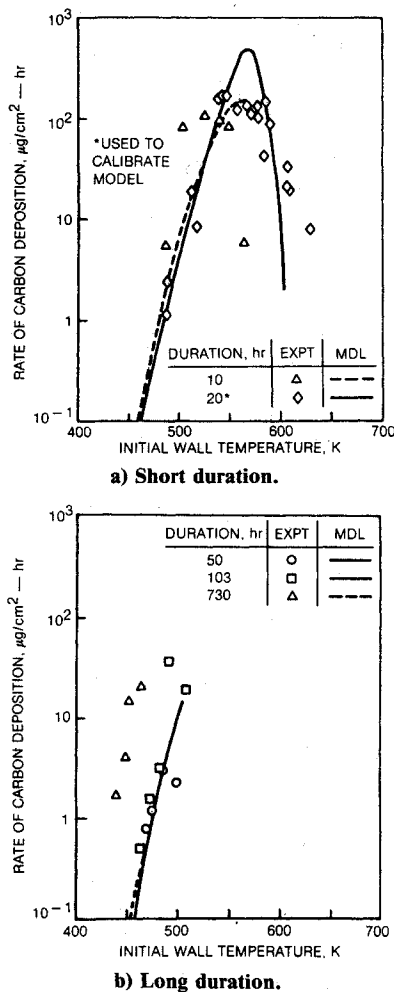


Fig. 9 Predicted and measured carbon deposition rates for Jet A at low velocity (0.07 m/s).

crements and marching in time along the length of the tube, where the time increment is computed from the specified tube incremental length and the local fuel velocity. Thus, given the wall and fuel temperature profiles along the tube, the test duration, fuel flow rate, initial concentration of oxygen in the fuel ( $[O_2]_0$ ), and pre-exponential and activation energy constants, the fuel oxidation and deposition model integrates Eqs. (3-5) to produce the concentrations (and total masses) of the oxygen, precursor, and deposit along the tube.

Figure 8 summarizes some predicted species concentration profiles and the total accumulated deposit along the tube for Jet A. In Fig. 8a, the total deposit produced for the high-temperature, low-velocity condition does not increase significantly downstream of 70 cm (because of suspected oxygen depletion). These data provided a convenient point for setting the value of  $[O_2]_0$ . Also, at this condition, the model predicts that the precursor concentration reaches a maximum value prior to a significant depletion of the oxygen and, during precursor formation, the local deposit concentration is nearly proportional to precursor concentration. However, once the oxygen concentration is significantly reduced, the previously formed precursor is converted to deposit. Further, when the model is applied to the low-temperature, low-velocity condition shown in Fig. 8b, the total deposit formed under these conditions is limited by the maximum tube temperature rather than by the oxygen concentration.

The predictive capability of the fuel oxidation and deposition model for a range of temperature conditions and flow

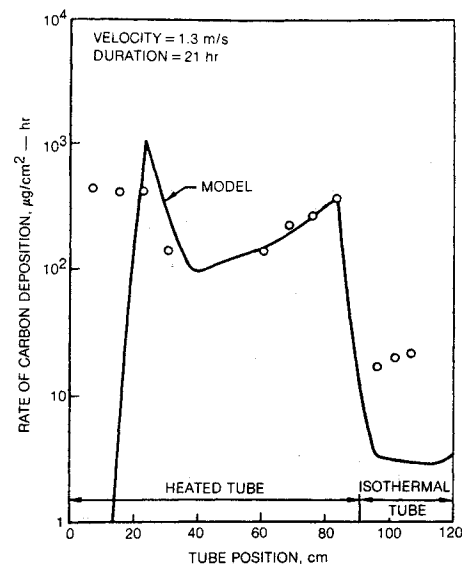


Fig. 10 Predicted and measured carbon deposition rates for Jet A at high velocity.

rates is demonstrated in Fig. 9 for several short- and long-duration tests at low-velocity and in Fig. 10 for a high-temperature, short-duration test at high velocity. The predicted and experimentally determined rates of carbon deposition of heated tubes are plotted vs the initial wall temperature (Fig. 9) and tube position (Fig. 10). As shown by Figs. 9 and 10, the agreement between the model and the experiment is satisfactory for the extreme ranges of flow rates and wall temperatures and for test durations that do not exceed 103 h. However, since the model does not account for either the enhancement effect on the deposit formation of an increase in the active surface area provided by extremely thick and cellular deposits or in the temperature gradients that develop in thick deposits over long durations, it does not match the experimental data for tests with durations longer than 103 h (Fig. 9). Also, as shown in Fig. 10, the model correctly predicts that the deposit rate increase for the region of tube between 40 and 80 cm, and it suggests that this is because the oxygen in the fuel is not significantly depleted during the relatively short time the fuel is in the tube (about 0.9 s).

## Conclusions

- 1) Local deposit formation is primarily a function of local surface temperature, but fuel temperature-time history can have a significant effect.
- 2) The rates of carbon deposition are similar at low (0.07 m/s) and high (1.3 m/s) velocity, but the deposit density varies by a factor of 10 for these extremes.
- 3) The time-averaged-rates of carbon deposition for deposits that are cellular in structure are not constant and increase with approximately the second power of the test duration. The increase is probably due to the additional surface area provided by the deposit.
- 4) A two-step kinetic model has been used to model the fuel oxidation and deposit formation process and to correlate deposit formation as a function of test time, surface temperature, and fuel temperature-time history.

## Acknowledgment

This work was performed with the support of the NASA Lewis Research Center, under Contract NAS3-24091, S. Cohen, Project Manager.

### References

<sup>1</sup>Szetela, E. J., Giovanetti, A. J., and Cohen S., "Fuel Deposit Characteristics at Low Velocity," ASME Paper 85-IGT-130, Sept. 1985.

<sup>2</sup>Bradley, R., Bankhead, R. and Bucher, W., "High Temperature Hydrocarbon Fuels Research in an Advanced Aircraft Fuel System Simulator on Fuel AFFB-14-70," AFAPL-TR-73-95, April 1974.

<sup>3</sup>Faith, L. E., Ackerman, G. H. and Henderson, H. T., "Heat Sink Capability of Jet A Fuel: Heat Transfer and Coking Studies," NASA CR-72951, July 1971.

<sup>4</sup>Giovanetti, A. J. and Szetela, E. J., "Long Term Deposit Formation in Aviation Turbine Fuel at Elevated Temperature," Final Rept. NASA Contract NAS3-24091.

<sup>5</sup>"CRC Literature Survey on the Thermal Oxidation Stability of Jet Fuel," Coordinating Research Council, Inc., Atlanta, GA, CRC Rept. 590, April 1979.

<sup>6</sup>Hazlett, R. N., "Progress Report on Advanced Hydrocarbon Fuel Development," U.S. Naval Research Laboratory, March 1975; also, *Journal of Industrial and Engineering Chemistry*, Vol. 16, No. 2, 1977, pp. 171-177.

*From the AIAA Progress in Astronautics and Aeronautics Series . . .*

## **GASDYNAMICS OF DETONATIONS AND EXPLOSIONS—v. 75 and COMBUSTION IN REACTIVE SYSTEMS—v. 76**

*Edited by J. Ray Bowen, University of Wisconsin,  
N. Manson, Université de Poitiers,  
A. K. Oppenheim, University of California,  
and R. I. Soloukhin, BSSR Academy of Sciences*

The papers in Volumes 75 and 76 of this Series comprise, on a selective basis, the revised and edited manuscripts of the presentations made at the 7th International Colloquium on Gasdynamics of Explosions and Reactive Systems, held in Göttingen, Germany, in August 1979. In the general field of combustion and flames, the phenomena of explosions and detonations involve some of the most complex processes ever to challenge the combustion scientist or gasdynamicist, simply for the reason that *both* gasdynamics and chemical reaction kinetics occur in an interactive manner in a very short time.

It has been only in the past two decades or so that research in the field of explosion phenomena has made substantial progress, largely due to advances in fast-response solid-state instrumentation for diagnostic experimentation and high-capacity electronic digital computers for carrying out complex theoretical studies. As the pace of such explosion research quickened, it became evident to research scientists on a broad international scale that it would be desirable to hold a regular series of international conferences devoted specifically to this aspect of combustion science (which might equally be called a special aspect of fluid-mechanical science). As the series continued to develop over the years, the topics included such special phenomena as liquid- and solid-phase explosions, initiation and ignition, nonequilibrium processes, turbulence effects, propagation of explosive waves, the detailed gasdynamic structure of detonation waves, and so on. These topics, as well as others, are included in the present two volumes. Volume 75, *Gasdynamics of Detonations and Explosions*, covers wall and confinement effects, liquid- and solid-phase phenomena, and cellular structure of detonations; Volume 76, *Combustion in Reactive Systems*, covers nonequilibrium processes, ignition, turbulence, propagation phenomena, and detailed kinetic modeling. The two volumes are recommended to the attention not only of combustion scientists in general but also to those concerned with the evolving interdisciplinary field of reactive gasdynamics.

*Published in 1981, Volume 75—446 pp., 6×9, illus., \$35.00 Mem., \$55.00 List  
Volume 76—656 pp., 6×9, illus., \$35.00 Mem., \$55.00 List*

TO ORDER WRITE: Publications Dept., AIAA, 1633 Broadway, New York, N.Y. 10019